Radiation Damage Calculation by NPRIM Computer Code with JENDL3.3

Satoshi SHIMAKAWA[a,b], Naoto SEKIMURA[b] and Naoki NOJIRI[a]

[a] *Department of HTTR Project, Japan Atomic Energy Research Institute,*
3607 Oarai-machi, Higashi-ibaraki-gun, Ibaraki-ken, 311-1394 Japan
E-mail: shim@oarai.jaeri.go.jp, nojiri@oarai.jaeri.go.jp

[b] *Department of Quantum Engineering and Systems Science, University of Tokyo,*
7-3-1 Hongo, Bunkyo-ku, Tokyo,113-8656 Japan
E-mail: sekimura@q.t.u-tokyo.ac.jp

The Neutron Damage Evaluation Group of the Atomic Energy Society of Japan starts an identification of neutron-induced radiation damage in materials for typical neutron fields. For this study, a computer code, NPRIM, has been developed to be free from a tedious computational effort, which has been devoted to the calculation of derived quantities such as dpa and helium production rate. Neutron cross sections concerning to damage reactions based on JENDL3.3 are given with 640-group-structure. The impact of cross sections based on JENDL3.3 to damage calculation results has been described in this paper.

1. Introduction

Within the framework of the neutron damage evaluation group in the Atomic Energy Society of Japan a study is under way to evaluate neutron induced radiation damage under several neutron fields of power reactors, material testing reactors and future fusion reactors. Various types of neutron irradiation tests will be proposed and designed to solve materials issues and develop new materials using research and testing reactors. There is a strong requirement to have more reliable parameters for irradiation tests from materials research users; however, there is no convenient tool to provide guide for damage correlation between different neutron environments. A computer code NPRIM [1] has been developed to provide a convenient way to calculate damage parameters such as dpa. Several neutron spectra are prepared as typical neutron fields, such as the JMTR [2], HTTR [3], YAYOI [4], JOYO [5], HFIR [6], ATR [7] and DT fusion [8].

In this paper, the impact of cross sections based on JENDL3.3, JENDL3.2, JENDL3.1, ENDF/B-VI, ENDF/B-V and ENDF/B-IV, to damage calculation results has been described using NPRIM code.

2. Specification of NPRIM

The NPRIM code, which can be obtained from the Internet site (http://marie.q.t.u-tokyo.ac.jp/nprim/), works with a graphical user interface (GUI) on PC platforms of Windows or Macintosh. Therefore, users do not need a lot of operation skills to use a workstation or mainframe computer. Calculation results of NPRIM code include energy-dependent and reaction-dependent dpa (displacement per atom), and gas productions, such as He appm (atomic parts per million of helium). The longstanding spectral indices, such as fast neutron fluence (E>1.0 or >0.1MeV) and others, are also calculated. Cross section sets and sample neutron spectra are bundled in the code. To evaluate radiation damage, users are only required to specify a neutron spectrum with free energy structure.

Neutron spectrum input is allowed in free energy structure. The input energy structure is automatically transformed to 640 groups and the quantities concerning to neutron irradiation are calculated with the energy dependent cross sections. The output energy structure can be also selected from the bundled sets or a user defined structure.

3. Processing of neutron cross sections

Cross sections of damage energy production and helium gas production are generated from the nuclear data file of JENDL3.3 [9] by the nuclear processing code NJOY 99.32. In the NJOY code [10], point wise cross section is re-processed by the BROADR module to adopt a Doppler broadening effect. The HEATR module is used to calculate the cross sections of damage energy production and helium production. Robinson's numerical approximation to the Lindhard partition function is implemented in the HEATR module for displacement model. The GROUPR module is used to convert into a fine group structure (SAND-IIA: 640 group structure) with the weighting function of fission spectrum, 1/E slow-down spectrum and Maxwellian thermal spectrum. The cross sections for the energy range from 10^{-10} to 20 MeV are as the cross section sets in the NPRIM code.

A damage energy production cross section represents the probability that atoms are displaced from initial lattice positions by collisions initiated from a neutron of a specified energy. In the NPRIM calculation, the damage energy production cross section, σ_D, is converted to the dpa cross section, σ_{dpa}, as

$$\sigma_{dpa}(E) = \frac{0.8}{2Ed}\sigma_D(E) \tag{1}$$

where Ed, named displacement energy, is the threshold energy for knock-on atom displaced from its lattice position. The value of Ed in iron has been selected as 40eV. Four reaction types of damage energy production cross sections, the total, elastic scattering, inelastic scattering and disappearance, are stored into the cross section set. The disappearance reaction is represented as summation of (n,γ), (n,α), (n,p) and other charged particle production cross sections.

The helium production cross section, σ_{He}, is generated from a total alpha production cross section (MT number=207 in the JENDL3.3) and also stored into the cross section set. Therefore, σ_{He} is a summation of the cross sections of (n,α), (n,nα), (n,2α), (n,3α) and other alpha production reaction, as follows.

$$\sigma_{He}(E) = \sigma_{n,a}(E) + \sigma_{n,na}(E) + 2\sigma_{n,2a}(E) + 3\sigma_{n,3a}(E) + ... \tag{2}$$

To compare the calculation results, other cross section sets such as the ASTM E693-94 [11], ENDF/B-V of the SPECTER [12], JENDL3.1 of the TENJIN [13], JENDL3.2 of the NPRIM and the new standard of ASTM E693-01 [14] based on ENDF/B-VI are also prepared.

4. Impact of cross sections

4.1. dpa of iron

Trial dpa calculations for a pure iron under neutron irradiation in several reactors are performed with various cross section sets. Table 1 compares the calculated results by the NPRIM code for 100 effective full power days in fission reactors, at the irradiation holes in the HTTR, JMTR, JOYO, at the core region in the PWR and BWR, and at the first wall for the DT fusion reactor (design phase of ITER).

For all the listed reactors, the dpa values using JENDL3.3 (NPRIM code) are good agreement with those using ENDF/B-V (SPECTER code), ENDF/B-IV (ASTM Standard E693-94) and ENDF/B-VI (new ASTM Standard E693-01). The difference of dpa shows slight overestimation by about 0 – 3% in the fission reactors. The values based on JENDL3.3 show good agreement within 2% compared with those of ENDF/B-V in the fission reactors. In the DT fusion reactor, the difference shows slight underestimation by about 1 – 3%. The calculated dpa values based on JENDL3.3 code, ENDF/B-V and ENDF/B-VI show reasonable agreement within 3%. On the other hands, dpa based on the JENDL3.3 is about 0 – 4% overestimation compared with the JENDL3.2-based one. Fig. 1 shows differences between the JENDL3.3 and JENDL3.2 dpa cross sections for natural iron. The resonance parameters of iron in the JENDL3.3 have been modified from JENDL3.2. Therefore, the dpa discrepancy in the fission reactors is mainly caused by the values of elastic cross section in the energy range from 1.5 to 800 keV.

Table 1. Calculation results of iron dpa compared with other codes.

Library (Code or Standard)	HTTR hole	JMTR hole	JOYO hole	PWR* core	BWR* core	DT first wall
JENDL3.3 (NPRIM)	0.0433	2.35	11.0	0.128	0.126	10.2
JENDL3.2 (NPRIM)	0.0419	2.29	10.6	0.125	0.123	10.2
ENDF/B-V (SPECTER)	0.0433	2.32	10.9	0.126	0.125	10.5
ENDF/B-IV (ASTM E693-94)	0.0428	2.31	10.7	0.126	0.125	10.4
ENDF/B-VI (ASTM E693-01)	0.0427	2.29	10.8	0.125	0.123	10.3

(unit in dpa; for 100 effective full power days) * Normalized to $1x10^{17}$ $m^{-2}s^{-1}$ (E>1.0MeV)

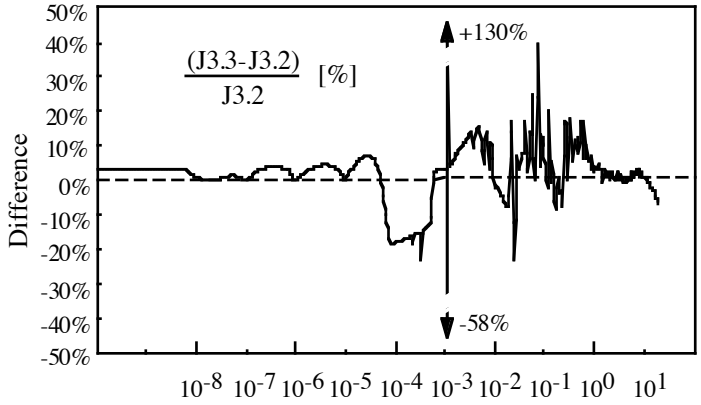

Fig. 1. Differences between the JENDL3.3 and JENDL3.2 dpa cross sections for natural iron

4.2. dpa rate and helium production rate of stainless steel

The dpa cross section for an austenitic stainless steel type 304 (304SS) is represented as atom-weighted summation of major elements. Chemical composition of the 304SS is assumed as iron of 71.8 wt-%, nickel of 9.3 wt-% and chromium of 18.9 wt-%, and other minor elements and impurities, such as C, Si, Mn, P, Cu, Nb, V, N, Co and B, are ignored in this calculation. Fig.2 shows dpa cross section of stainless steel type 304 using NPRIM code with JENDL3.3, comparing with one of natural iron using ASTM E693-94.

Table 2 shows the results of dpa rate (dpa/s) using JENDL3.3 for 304SS in several reactors, comparing with those using ENDF/B-V in the SPECTER code. The dpa rate using JENDL3.3 differs by –3% from those using ENDF/B-V. Especially, concerning to the dpa rates of the listed fission reactors, it is found that the values using JENDL3.3 show in excellent agreement with those using ENDF/B-V, within 0.6%.

Helium production rates in the 304SS are summarized in Table 2. With aging of power reactors, degradation of weldability caused by helium bubble formation on grain boundaries in austenitic steels has become one of the problems to maintain the irradiated structure materials [15]. Therefore, it is important to evaluate of helium production as accurate as possible. In Table 2, these values do not include the two-step helium productions through $^{58}Ni(n,\gamma)^{59}Ni(n,\alpha)^{56}Fe$ reaction by low energy neutrons. The value of helium production rate using JENDL3.3 in the material testing reactors, i.e. the JMTR and JOYO, differs by about 10% from those using ENDF/B-V.

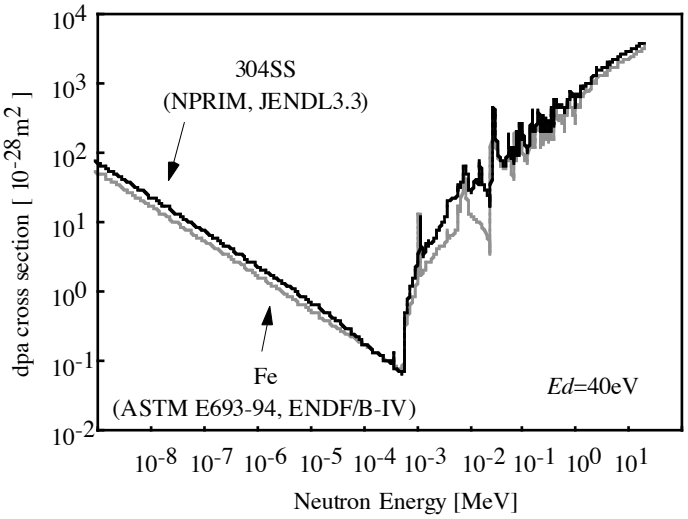

Fig. 2. dpa cross section for 304SS (JENDL3.3,NPRIM) and iron (ENDF/B-IV,ASTM)

Table 2. Calculation results of dpa and He production rate for 304SS in several reactors.

Library (Code)	HTTR hole	JMTR hole	JOYO hole	PWR* core	BWR* core	DT first wall
dpa rate (unit in x10^{-7} dpa/s)						
JENDL3.3 (NPRIM)	0.0523	2.76	13.1	0.150	0.148	11.9
ENDF/B-V (SPECTER)	0.0527	2.76	13.0	0.150	0.148	12.2
difference	*-0.6%*	*<0.1%*	*+0.4%*	*<0.1%*	*-0.1%*	*-3%*
He production rate (unit in x10^{-8} He appm/s)						
JENDL3.3 (NPRIM)	0.272	14.3	42.2	1.39	1.38	1320
ENDF/B-V (SPECTER)	0.283	13.2	38.1	1.38	1.36	1580
difference	*-4%*	*+9%*	*+11%*	*+0.7%*	*+0.9%*	*-17%*

* Normalized to 1x10^{17} $m^{-2}s^{-1}$ (E>1.0MeV)

4.3. Damage attenuation through pressure vessel of PWR and BWR.

The attenuations of dpa rate and helium production rate through the pressure vessel (RPV) of the PWR and BWR are calculated using the NPRIM code with the JENDL3.3. The chemical composition of the RPVs is assumed to 100% iron. To estimate the spectrum dependence of helium production, typical boron impurity level of 11 wt.ppm is also considered. The 99 group neutron spectra [16] are specified in the water, at 1/4 and 3/4 of RPV thickness, and in the cavity. The spectra at the 1/4 T and 3/4 T of the RPV are shown in Fig.3.

Figure 4 shows the calculated dpa rate attenuation. Two kinds of fast neutron flux, such as $\phi_{0.1}$ of E > 0.1MeV and $\phi_{1.0}$ of E > 1MeV, are also plotted in this figure. Significant differences are identified for the attenuation ratio of the $\phi_{0.1}$, compared with dpa rate in the RPV of PWR and BWR. It seems that the attenuation profiles of the $\phi_{1.0}$ are similar to the dpa rate, however, the $\phi_{1.0}$ attenuation ratios at 3/4 T of the RPV are about 56% and 79% of dpa rate in the PWR and BWR, respectively. The calculated helium production rate attenuations are shown in Fig.5. Contribution of two-step helium productions by $^{58}Ni(n,\gamma)^{59}Ni(n,\alpha)^{56}Fe$ reaction is negligible compared with those from the direct productions of Fe, Ni and Cr, because of the low neutron flux at the RPV. The attenuation profiles of the helium production with $^{10}B(n,\alpha)$ reaction are not similar to those without B. Note that the differences between the attenuation rates with and without boron are as almost ten times in the RPV.

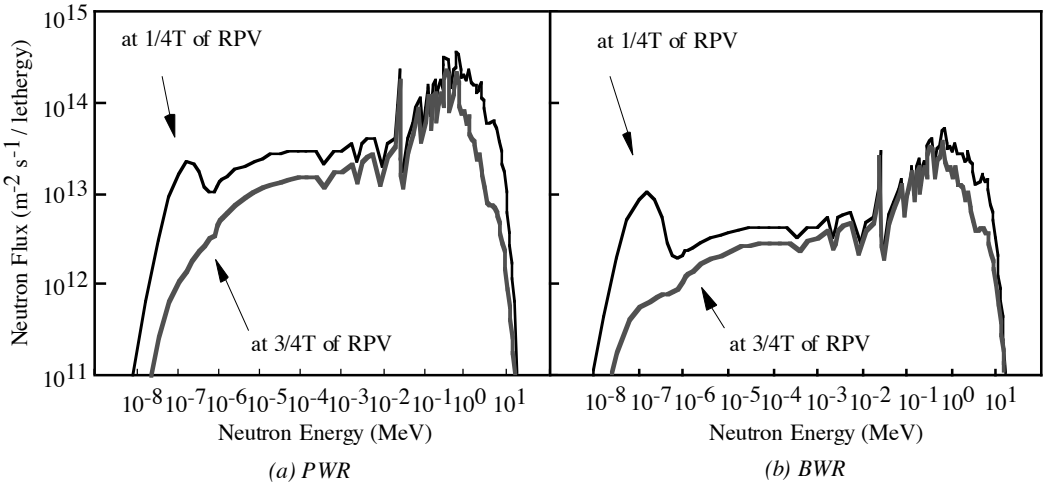

Fig. 3. Neutron Spectra in RPV of PWR and BWR

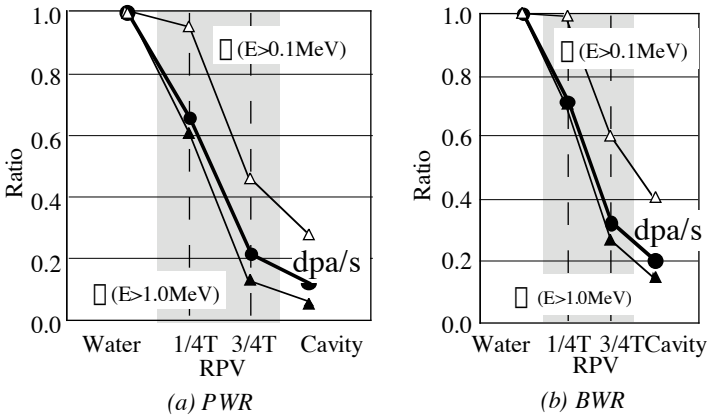

Fig. 4. Attenuation of neutron flux and dpa rate through RPV in PWR and BWR.

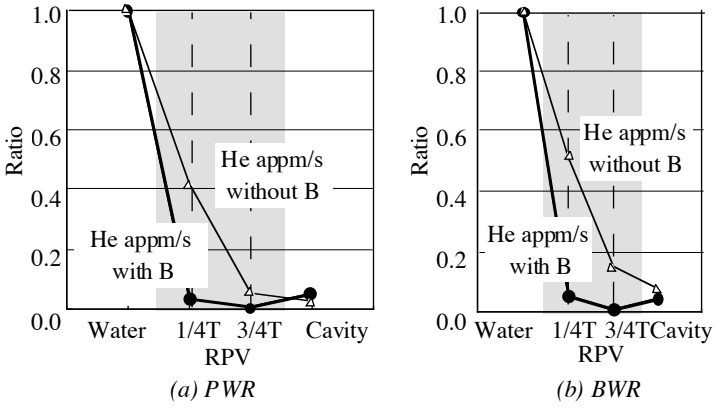

Fig. 5. Attenuation of Helium production rate through RPV in PWR and BWR.

Figure 6 shows the impact of cross sections on dpa rate determination through the RPV of the PWR and BWR. In this figure, the calculation results using JENDL3.2 shows good agreemant, about 1% lower through the RPV, with one using ENDF/B-IV in the ASTM Standard E693-94. The dpa rate using JENDL3.3 in the NPRIM code, ENDF/B-V in the

SPECTER code and ENDF/B-VI in new ASTM Standard E693-01 are almost same, and each difference from one using ENDF/B-IV in the ASTM Standard E693-94 becomes lager at the outer position of the RPV. All results of dpa rate indicate good agreement within 6%.

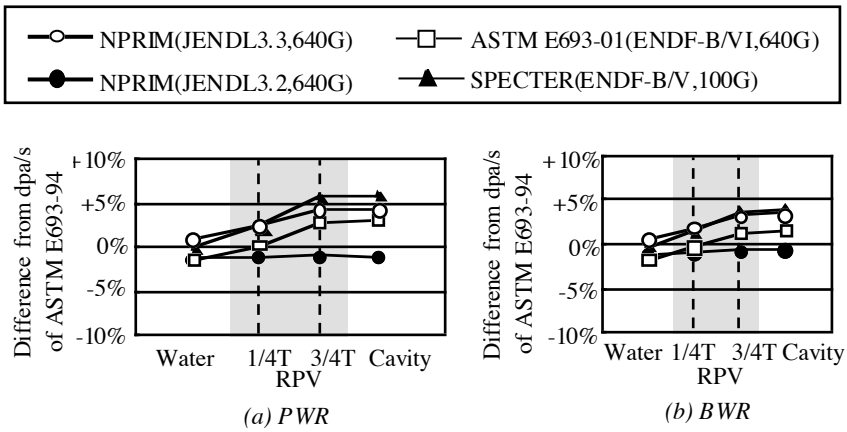

Fig. 6. Impact of cross sections on RPV dpa rate determination.

5. Summary

The comparison of the calculation results for iron dpa between the NPRIM code with neutron cross section set based on the JENDL3.3, ASTM Standard E693 based on ENDF/B-IV and SPECTER codes based on ENDF/B-V shows good agreement in six kinds of neutron fields of the HTTR, JMTR, JOYO, PWR, BWR and DT fusion. For neutron irradiation of austenitic stainless steel, no significant difference for dpa rates using JENDL3.3 indicates in comparing with those using ENDF/B-V for the six kinds of neutron fields. The results of dpa rate calculation through the RPV of the PWR and BWR using various cross section libraries, JENDL3.2, JENDL3.3, ENDF/B-V and ENDF/B-VI**,** indicate good agreement about 6% with one using ENDF/B-IV of ASTM E693-94.

References

[1] S. Shimakawa and N. Sekimura, J. Nucl. Mater. (2001) in printing
[2] S. Shimakawa, ASTM STP 1398, (2000) 244
[3] K.Yamashita, J, Nucl. Sci. Eng. 122, (1996) 212.
[4] M.Nakazawa, T.Taniguchi, M.Kato, A.Sekiguchi, K.Kobayashi, K.Sakurai, and S.Suzuki, UTNL-R 0037 (1976)
[5] T.Sekine, T. Aoyama, A.Yoshida and S.Suzuki. ASTM STP 1398, (2000) 268
[6] K.R. Thoms and A.F. Rowcliffe, Journal of Neutron. Research Vol.2, No.2, (1994) 71.
[7] J.W.Rogers and R.A.Anderl, INEL-95/0494 (1995)
[8] S. Shimakawa et al., Fusion Eng. Des. 28 (1995) 215-219
[9] JAERI Nuclear Data Center: "Japanese Evaluated Nuclear Data Library Version 3 Revision 3 (JENDL-3.3)", private communication (2002).
[10] R. E. MacFarlane and D.W. Muir, LA-12740-M, (1994)
[11] ASTM recommended practice E693-94, Annual Book of ASTM Standard, Part 45 (1994)
[12] L.R.Greenwood and R.K.Smither, IAEA-TECDOC-263 (1985)
[13] K.Sone and K.Shiraishi, JAERI-M 6358 (1975)
[14] ASTM recommended practice E693-01, Annual Book of ASTM Standard, Part 45 (2001)
[15] K.Asano, S.Nishimura, Y.Sato, H.sakamoto, Y.Yamada, T.Kato and T.Hashimoto, J. Nucl. Mater. 264(1999) 1-9.
[16] L.R.Greenwood, private communication (2002)